EXAMPLES OF BOND GRAPH ASSISTED DYNAMIC SYSTEM DESIGN

Robin C. Redfield
Department of Engineering Mechanics
United States Air Force Academy
Colorado Springs, CO 80919
RedfieldRC.Dfem@Usafa.Af.Mil

KEYWORDS
Bond graphs, dynamic systems, design

ABSTRACT
Dynamic systems design requires configurations of component parts to provide specified relationships between dynamic or static variables. Bond graphs are the modeling medium that affords dynamics system design based mostly on frequency response, input-output specifications. Three example designs and perhaps novel systems are generated: an inertial velocity sensor, an inclinometer, and a continuously variable transmission. This work is a compilation and an extension of previous work in dynamic systems design.

BACKGROUND
The theme of this work is the applicability and utility of bond graphs in the conceptual or configurational design of dynamic systems. Design results for three different engineering systems are examined: inertial velocity sensors, inclinometers, and continuously variable transmissions. All three devices have various implementations as state of the art. Current implementations of velocity sensors are not particularly acceptable and hence not used much, if at all, in practice. Hence novel designs would be welcome. Inclinometers do exist and some work well. The test for the bond graph approach here is to generate possible new designs or to generate concepts that are already good. Continuously variable transmissions (CVTs) have many current implementations but none are satisfactory for high power requirements. New designs that can handle the power would be worthwhile.

Bond graphs have been used in conceptual design for the last ten years. Some work has been in using Bond Graphs for generating alternative designs since any part of a Bond Graph can be physically realized in a number of different energetic domains. Finger and Rinderle (1989) and Redfield and Krishnan (1993) deal at least in part with finding equivalent systems to known designs to "spark" novel solutions. Designing systems based on dynamic performance specifications involves specifying input-output requirements and formulating systems or subsystems of given systems to meet the requirements. This is the mechanical realization of network synthesis, Baher (1984).

Ulrich and Seering (1989) use static elements to generate steady state designs and Redfield (1992) and Redfield and Krishnan (1993) synthesize dynamic elements to meet frequency response specifications for novel dynamic systems.

The rest of the paper steps through using bond graphs to generate novel design concepts for a inertial velocity sensor, and inclinometer, and a continuously variable transmission. We use ideas of equivalent systems and system synthesis. Each generated concept is examined in little to moderate detail. Along the way concepts are suggested that may be new or old, and some that may be worth further study. The point is that bond graphs aided in generating starting points that would not have been easily possible otherwise.

The work in not unlike electrical network synthesis techniques but it is posed in a bond graph framework and shows promising results in generating novel designs for important systems. This paper is partially a compilation of previous work by the author augmented by extensions to that work. Three design scenarios are shown together in this paper to lend evidence to the utility of bond graphs in the design process.

INERTIAL VELOCITY INDICATOR
Inertial velocities are typically measured by either integrating an accelerometer signal or using grounded sensors such as the linear velocity transducer. More rarely they are obtained by differentiating position information. Velocimeters are not widely used because these seismic instruments have either 1) a narrow frequency band where both amplitude and phase are satisfactorily flat, or 2) only a high frequency range where the gain is low, or 3) a band pass measurement range that requires very large damping (Cannon, 1967; Doeblin, 1975).

To investigate possible designs for velocity meters we start with the configuration of Figure 1 which is somewhat arbitrary. Assume velocity V is to be measured with a sensor initially consisting of a mass suspended by a spring. The displacement of the spring is desired to be an indication of the velocity V. This initial configuration is perhaps motivated by the authors experience with seismic sensors where a proof mass is suspended in a case and its relative

displacement or motion is a measure of the inertial case motion. From a more fundamental view however, assume the author was ignorant of traditional seismic sensors. Desiring to measure an inertial velocity, we attach an arbitrary system to the moving object with some variable that we know can be measured (in this case a relative displacement). We then posit the addition of unknown elements that may alter to final dynamics favorably for our purposes.

In this example, an unknown dynamic system is to be added in parallel to the spring such that spring displacement is some measure of *V*. The unknown system could also have been added in series with the spring or attached to the proof mass alone perhaps. These alternatives are not examined here.
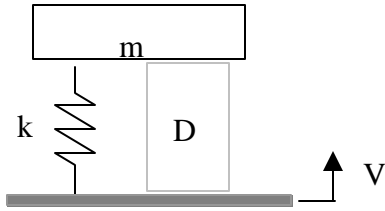

Figure 1 – Schematic of initial velocity meter configuration

The bond graph of this configuration is in Figure 2 and shows the velocity source with the initial mass and spring. The unknown subsystem, *D*, is shown in parallel with the spring and thus sharing the same relative velocity. The bonds are numbered to refer to specific power variables.
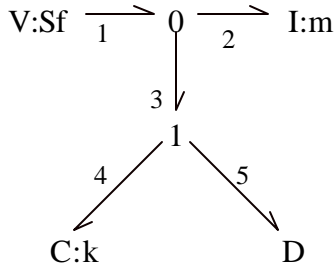

Figure 2 – Bond graph for velocity meter

If we determine the transfer function between the input velocity, f_1 and the spring displacement, q_4 using any method (one is shown by Redfield and Krishnan, 1993), equation 1 is developed.

$$\frac{q_4(s)}{f_1(s)} = \frac{ms}{ms^2 + D(s)s + k} \tag{1}$$

If we require the resulting frequency response to be flat for all frequency, algebra shows that

$$D(s) = -ms + m - \frac{k}{s} \tag{2}$$

This Laplace realization indicates that the unknown subsystem need consist of a negative mass and spring, and a positive damper all in series with the original spring. The negative spring is not a problem for two reasons. The first is that it would simply cancel the original spring. The design requires no spring at all. The second is that negative compliances are possible to construct. An inverted pendulum and a light switch are two examples. As long as these negative (unstable) elements are in an overall stable system, their motion will remain small. The negative mass is problematic however. A negative mass would be one where a positive momentum results in a negative velocity. The author is not aware of any such device.

We can get around the requirement for a negative mass by relaxing the requirement of our sensor and to only measure velocities below a certain frequency. If the new specification between spring displacement and input velocity is as in equation 3, the sensor will have a steady state gain of *G* and a break frequency of $1/\tau$.

$$\left(\frac{q_4(s)}{f_1(s)}\right)_{spec} = \frac{G}{\boldsymbol{t}s+1} \tag{3}$$

Putting this together with equation 1 results in the following Laplace representation for the unknown system (equation 4). There still is the negative spring that will cancel the original spring but now there is a positive damper and a positive mass as long as $\tau > G$.

$$D(s) = \frac{m(\boldsymbol{t}-G)}{G}s + \frac{m}{G} - \frac{k}{s} \tag{4}$$

The bond graph realization of this design is shown in Figure 3. The spring has been removed and a damper and mass have been placed at the relative velocity between the measured and proof mass.
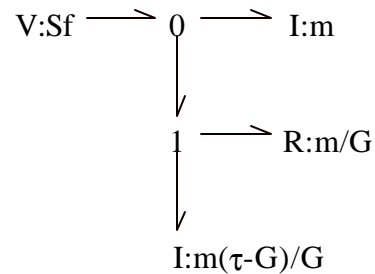

Figure 3 – Bond graph of velocity sensor

The physical realization of this velocity sensor is shown in Figure 4. Note how a mass that inertially responds to a relative velocity is found in the rotational inertia. The angular velocity of the rotating mass in a function of the

difference of the two translational inertias and its radius. This would not be possible with a translational mass where issues of nodicity come into play in an interesting way (Won and Hogan, 1999).
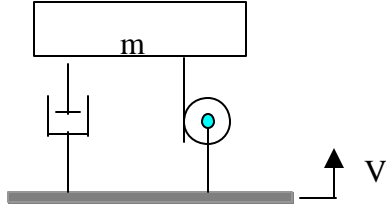

Figure 4 – Schematic of velocity sensor

One potential problem with the sensor of Figure 4 is its self collapsing nature and lack of equilibrium position. In the presence of a gravitational field or if its initial position was at a limit of motion, the sensor may not perform for all motion. Considering these practicalities, we leave the initial spring in place and simply leave our unknown system as the mass and damper in parallel without the negative compliance (equation 5).

$$D(s) = m_D s + b_D \qquad (5)$$

This results in the input-output performance of equation 6 where the lowest frequencies are now not measured.

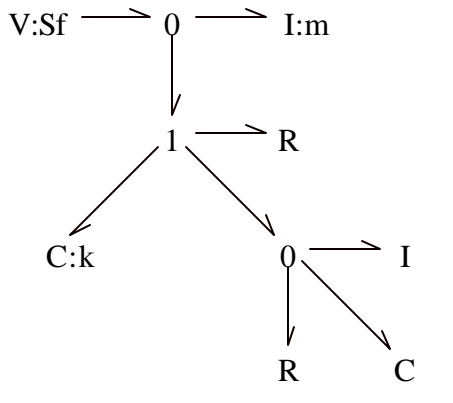$$\frac{q_4(s)}{f_1(s)} = \frac{ms}{(m+m_D)s^2 + b_D s + k} \qquad (6)$$

Figure 5 - Higher order sensor bond graph

This new performance is that of a band pass filter where its amplitude and phase tracking are quite limited between the break frequencies. Improved sensor performance is afforded by complicating the sensor with multiple poles at each of the break frequencies. Without the details, the bond graph of

the 4th order sensor is in Figure 5 and its schematic in Figure 6

This phase performance is markedly improved between the break frequencies. More specific performance can be found in Redfield, 1993.
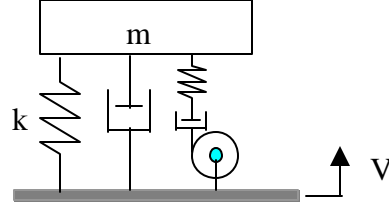

Figure 6 – Schematic of 4th order velocity sensor

INCLINOMETER

The next design example is that of an inclinometer or tiltmeter. These devices are meant to measure very small angles away from the horizontal. They can measure deflections in stiff structures such as the floors in buildings and they can measure "earth tide", the deflection of the earth's crust due to the gravitational attraction of the moon.

We will follow the same procedure as in the velocity sensor example where a starting configuration is augmented with additional dynamics to meet required input-output specifications. The starting point is again somewhat arbitrary but is certainly driven by a priori knowledge. It must be admitted up front that the author was initially aware of a very clever device for measuring tilt, but he did not know if the bond graph design approach would results in anything like the clever device. Bias and experience certainly play in parallel with the bond graph tool.

The initial configuration is shown in Figure 7 and is not unlike the starting point for the velocity sensor. A pendulum is mounted in a casing which is subject to small angles of tilt, φ. The casing height is L and the pendulum has length r. The pendulum angle relative to the casing, θ, is desired to be a measure of the tilt and indeed it is for low frequency and with a gain of one.
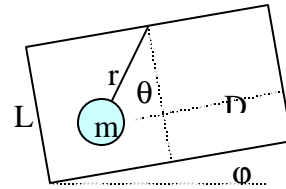

Figure 7 – Starting point for tiltmeter

It is desired to add a subsystem to the horizontal motion of the pendulum to increase the gain of the device and investigate the frequency response. Another possibility that was not pursued in this paper is to add dynamics to the relative angular motion of the pendulum.

Without including the details that can be found in Redfield and Krishnan, 1992, the bond graph based on the kinematics of the system for small angles is shown in Figure 8
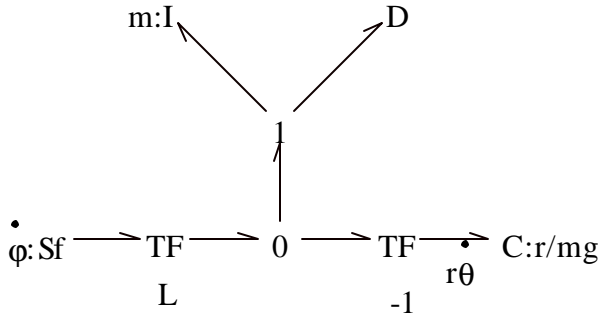

Figure 8 – Initial tilt meter bond graph

The input tilt is a source of flow on the left, the gravitational restoring force acts as a spring and is on the right, and the mass and unknown design, D, are attached to the horizontal velocity of the mass. The transfer function between the tilt and the pendulum angle is in equation 7 as a function of the parameters and the design impedance.

$$\frac{\boldsymbol{q}(s)}{\boldsymbol{j}(s)} = \frac{-L[ms^2 + D(s)s]}{rms^2 + rD(s)s + mg} \quad (7)$$

A number of iterations are possible examining both the specification θ/φ, and the design, D, but only a couple of the promising ones with be detailed here. The transfer function of equation 7 reveals that if D has the character of a compliance then

$$D(s) = \frac{k_D}{s} \quad (8)$$

and θ/φ will be constant in the steady state. For this design the I/O transfer function becomes

$$\frac{\boldsymbol{q}(s)}{\boldsymbol{j}(s)} = \frac{-L[ms^2 + k_D]}{rms^2 + rk_D + mg} \quad (9)$$

which is a pair of undamped zeroes over a pair of undamped poles. The gain at high frequency is constant at –L/r and at low frequency becomes

$$\left.\frac{\boldsymbol{q}(jw)}{\boldsymbol{j}(jw)}\right|_{w=0} = \frac{-Lk_D}{rk_D + mg} \quad (10)$$

Focusing on the dc (low frequency) behavior we see that large k_D, large L, small r and small m all add to the gain assuming all parameters are positive.

To "build" this design we pick an "infinite" spring, $k_D \rightarrow \infty$ (rigid connection) and form an approximate ground connection for the "spring" since no actual ground connection would be easily available if the earth's crust is

moving. Figure 9 shows the author's rendition of this system where the "ground" is a pendulum, G, that is attached to the casing. If $G>>m$, as the case rotates the ground pendulum stays nearly vertical and the kinematic linkage affords the gain between θ and φ.
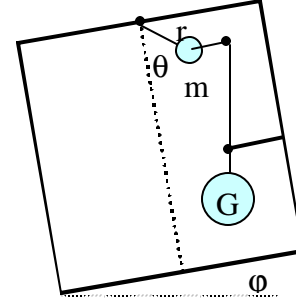

Figure 9 – Kinematic tiltmeter

It is certainly admitted that experience played a significant roll in coming to this design, but the bond graph and frequency response obviously lead the way in directing which relationships were necessary.

Equation 11 shows that another way for the sensor to exhibit high gain is for $r<0$ or for

$$k_D \rightarrow \frac{-mg}{r} \quad (11)$$

Focusing on the second possibility, a negative spring attached to the pendulum will allow the gain to approach infinity (see equation 10). Again from experience, an inverted pendulum is persuaded to perform the task and the design becomes that of Figure 10
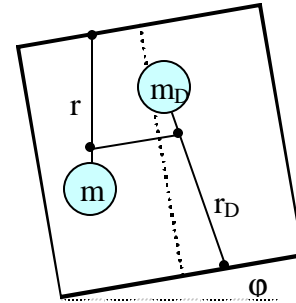

Figure 10 – Alternative tiltmeter concept

By adjusting the stiffness of the inverted pendulum relative to that of the first pendulum, the dc gain of pendulum angle relative to ground angle can approach infinity. As the gain grows, equation 9 shows that the poles of the system head towards zero so only dc response is possible.

This opposed pendulum configuration is the clever design that was fore-known to the author where a detailed discussion is available in Li and Jansson, 1980. It is not fair to say that this design would certainly have been arrived at

without prior knowledge, but the author would not be surprise if this had been the case.

CONTINUOUSLY VARIABLE TRANSMISSION

The last example of assisted design synthesis is that of a continuously variable transmission. In Bond Graph notation, the configuration design of a power transmission system would be shown as in Figure 11 Power enters on bond 1, is transformed through some yet unknown subsystem, *D*, and is output to bond 2 which is attached to a load impedance operator, I_L. Typically the load impedance would include an inertia and a resistance.

$$\xrightarrow{\quad 1 \quad} \mathbf{D} \xrightarrow{\quad 2 \quad} \mathbf{I_L}$$
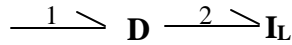
Figure 11 – Representation of power transformation

A number of approaches to this problem are in Redfield, 1999 but only some of the more promising will be shown with some additional results.

Standard approaches attempt to vary the gear ratio of a system with variable radii pulley with belts or friction wheels. The bond graph of such an arrangement is shown in Figure 12

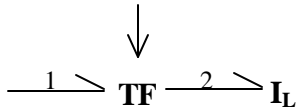$$\xrightarrow{\quad 1 \quad} \mathbf{TF} \xrightarrow{\quad 2 \quad} \mathbf{I_L}$$

Figure 12 – Transformer with variable modulus

Approaches using the concept of equivalent systems, (Karnopp et. al., 1990) recognize that serial gyrators function as a transformer as in Figure 13.
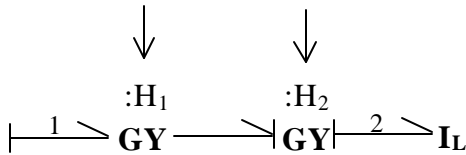
$$\vDash \xrightarrow{\quad 1 \quad} \overset{:H_1}{\mathbf{GY}} \longrightarrow \overset{:H_2}{\mathbf{GY}} \vDash \xrightarrow{\quad 2 \quad} \mathbf{I_L}$$

Figure – Mechanical gyrator realization

The transmission ratio would be the ratio gyrational modulli, $\dfrac{f_2}{f_1} = \dfrac{H_1}{H_2}$. This configuration can be physically realized mechanically, electro-mechanically, or hydro-mechanically. A pair of gyroscopes in series does the job mechanically although kinematic problems may be difficult or impossible to overcome. A generator-motor pair could create an electro-mechanical CVT with a wise choice of modulating parameters (Figure 14). Issues to examine are the power costs in the modulation and the practicality of implementation.
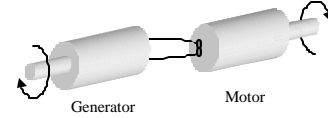

Figure 14 – Generator motor pair with variable field

In the hydro-mechanical transformation, centrifugal pumps act as gyrational elements converting torque to volumetric flow rate and angular velocity to pressure rise.   Series pumps could convert one angular velocity to another with the modulation occurring by varying vane geometry (Figure 15).   Some issues here are losses intrinsically associated with the pumps.
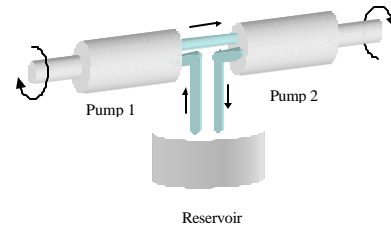

Figure 15 – Series centrifugal pumps

Other series designs can be considered but bond graphs with loops between the input and output can generate designs with more degrees of freedom in impedance choice as in Figure 16.
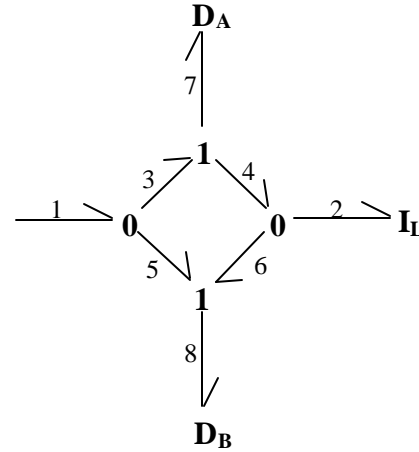

Figure 16 – Loopic configuration

To determine the input–output relationships, chosen variables are related directly from the graph assuming linear impedance operators (*D* and *I*). The variables are chosen assuming f_1 is an input, f_2 is the output and the flow on bond 7 and the input and output efforts are worth examining. Solving for the output flow gives the transfer function of equation 12. Immediately we can see that the design impedances can markedly affect the steady state performance.

$$\frac{f_2}{f_1} = \frac{D_B - D_A}{4I_L + D_B + D_A} \tag{12}$$

If the design impedances are resistive, significant power is probably dissipated although this should be examined in detail. If the design is inertial, the dc gain becomes zero. Other, more complicated possibilities can be considered but an interesting one is if both elements are capacitive ($D_A = k_A / s$ and $D_B = k_B / s$). For this case the flow ratio is shown in equation 13 where the load $I_L = ms + c$.

$$\frac{f_2}{f_1} = \frac{k_B / k_A - 1}{4(m/k_A)s^2 + 4(c/k_A)s + k_B / k_A + 1} \tag{13}$$

The dc ratio, N, can be varied from -1 to 1 by varying the stiffness ratio ($r = k_B / k_A$):

$$N = \frac{r-1}{r+1} \tag{14}$$

Figure 17 shows this relationship where the choice of r can give forward, neutral, and reverse! The flow ratio is also independent of load.
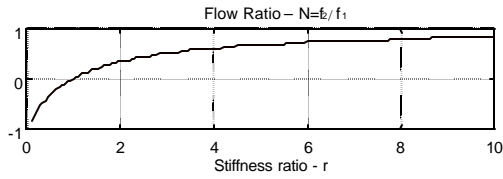

Figure 17 – Flow ratio as function of stiffness

This seems like an exciting result until we step back and realize that he capacitive elements wind up indefinitely thus storing increasing amount of energy. Thus the CVT performs well in terms of controlling the flow ratio, but the efficiency is poor as more and more energy goes into potential energy storage. Further study may determine how to tap that energy for useful work or channel it back into the system

The above examination can prompt one to consider other possibilities while trying to understand why the compliant elements worked to control the flow ratio. If sources replace the compliant elements to force the flow ratio to a desired value we get the bond graph of Figure 18.
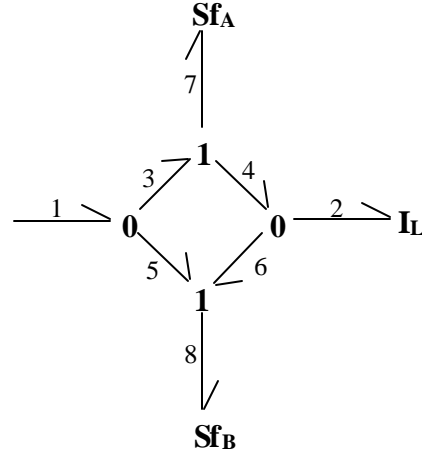

Figure 18 - Flow sources controlling flow ratio

Let N still be the I/O flow ratio. If we demand power in and out equal then $e_1 / e_2 = N$, the sources have equal and opposite power and a number of relationships develop. The control to I/O flow ratio is:

$$\frac{f_7}{f_1} = \frac{N+1}{2} \quad \text{and} \quad \frac{f_8}{f_1} = \frac{1-N}{2} \tag{15}$$

and the power ratios become

$$\frac{P_7}{P_1} = \frac{(N+1)(N-1)}{2N} \quad \text{and} \quad \frac{P_8}{P_1} = \frac{-(N+1)(N-1)}{2N} \tag{16}$$

The controlled powers on bond 7 and 8 are opposite in sign as required for power conservation. One question becomes how does the controlling flow ratio and power compare to the input/output power. If the power through the controlling elements is less than that through the input-output ports of the entire device, the result is a CVT power amplifier in the configuration of Figure 19.
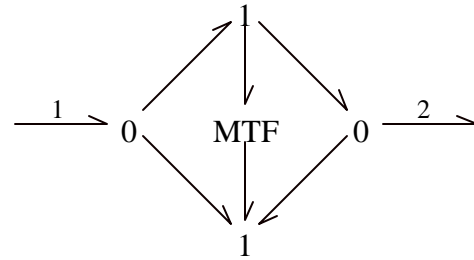

Figure 19 – CVT power amplifier

The modulated transformer (MTF) is a CVT that may handle lower power depending on the flow ratios required between ports 1 and 2. To examine this question, equations 16 and 15 are plotted in Figures 20 and 21 for examination.
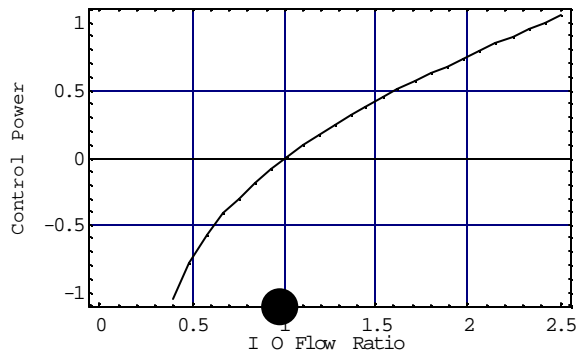
Figure 20 Control power vs. I/O power

Figure 20 shows the power ratio between the control (MTF) and the I/O as a function of flow ratio. Between flow ratios of 0.4 and 2.5, the control handles less power than I/O. This is potentially an important result because power capabilities are limiting the scope of CVT application.

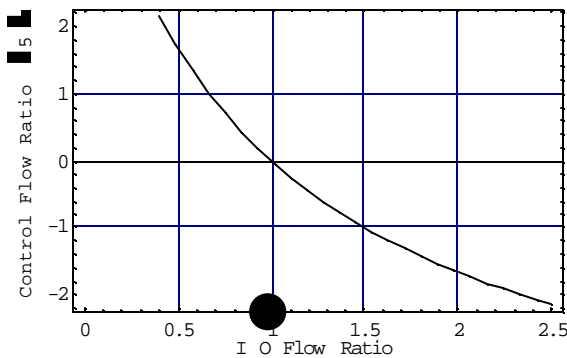Figure 21 shows the flow ratio in the control as a function of the I/O flow.

Figure 21 – Control to input power ratio

This figure scales the control flow by a factor of five so that a second stage amplifier can be used. Note how critical the I/O speed ratio is to the power used in the control (Figure 20). A two stage configuration is shown in Figure 22
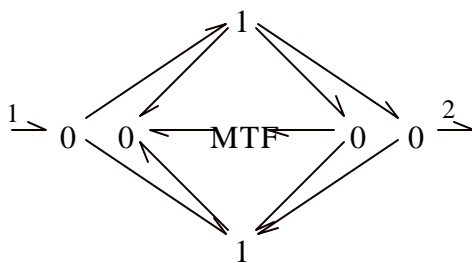

Figure 22 – Two stage CVT amplifier

and the power and flow requirements for the two stage device are shown in Figures 23 and 24
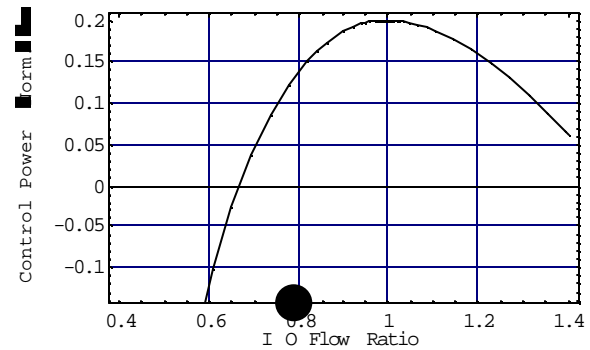

Figure 23 – Two-stage power requirements

Flow ratios of 0.6 to 1.4 can be controlled by modulating less than 20% of the I/O power. This is a significant gear range and a significant step down in power handled by the modulating device. Figure 24 shows the flow ratios necessary by the controlling module which of course could be scaled by some fixed gearing as before
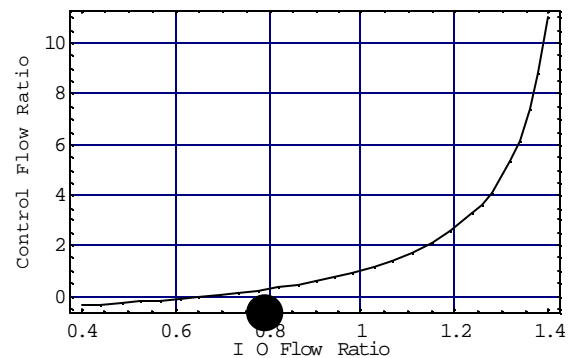

Figure 24 – Required flow ratio for two-stage amplifier

If the control element cannot handle a reversal of flow, the I/0 flow ratio could be, say, 0.8 to 1.4 with a control flow range of 1 to 11 as seen in the plot.

CONCLUSIONS

The work of this paper is to demonstrate the value of using bond graphs as a conceptual or configurational design tool for dynamic systems. Three example designs were investigated only briefly but the utility of the tool was hopefully apparent.

This does not necessarily mean that any of the concepts will eventually be found feasible but they are concepts none-the-less that are worth further study. Much of design is by redesign and analogy. Redesign is related to systems that start with some initial configuration and may benefit from modification and augmentation. Analogy is pervasive in

bond graph modeling since bond graphs unify engineering systems based on power and energy.

The Bond Graph approach of this paper gives a tool to assist in design for the class of systems where the dynamic relations of the effort, flow, and/or power are the driving requirements. Some of these systems require further study and perhaps prototyping. None of this analysis was conducted exhaustively and other new ideas are likely still buried and awaiting discovery. An further area worth pursuing on the conceptual design side is the inclusion of nonlinear elements and specifications.

REFERENCES

Baher, H., 1984, *Synthesis of Electrical Networks*, Wiley, New York, NY.

Cannon, R. H., 1967, *Dynamics of Physical Systems*, McGraw-Hill, New York.

Doebelin, E. O., 1975, *Measurement Systems: Application and Design*, McGraw-Hill, New York.

Finger, S., and Rinderle, J. R., 1989, "A Transformational Approach to Mechanical Design Using a Bond Graph Grammar," In *Design Theory and Methodology-DTM '89*, DE-Vol. 17, pp. 107-116..

Karnopp, D, Margolis, D., and Rosenberg, R., 1990, *System Dynamics: A Unified Approach*, Wiley.

Redfield, Robin C. and Krishnan, S., 1992, "Towards Automated Conceptual Design of Physical Dynamic Systems," *Journal of Engineering Design*, Vol. 3, No. 3, pp. 187-204.

Redfield, Robin C. and Krishnan, S., 1993, "Dynamics System Synthesis with a Bond Graph Approach Part I – Synthesis of One-port Impedances," *J. of Dynamic Systems, Measurement and Control*, Vol. 115, No. 3, pp.357-363.

Redfield, Robin C., 1993, "Dynamic System Synthesis with a Bond Graph Approach Part II – Conceptual Design of an Inertial Velocity Indicator," *J. of Dynamics Systems, Measurement and Control*, Vol. 115, No. 3, pp.364-369.

Redfield, R. C., 1999, "Bond Graphs in Dynamic System Design: Concepts for a Continuously Variable Transmission," *1999 International Conference on Bond Graph Modeling an Simulation (ICBGM '99)*, The Society for Computer Simulation, Granda and Cellier editors, pp. 90-95.

Ulrich, K. T., and Seering, W. P.,1989, "Synthesis of Schematic Descriptions in Mechanical Design," *Research in Engineering Design*, Vol. 1, pp. 3.

Won, J. and Hogan, N, 1999, "Nodic and Non-nodic Structures in Physical Systems," *1999 International Conference on Bond Graph Modeling an Simulation (ICBGM '99)*, The Society for Computer Simulation, Granda and Cellier editors, pp. 90-95.